Recruitment of dynein to the Jurkat immunological synapse

Jeffrey Combs*, Soo Jin Kim*, Sarah Tan*, Lee A. Ligon†, Erika L. F. Holzbaur†, Jeffrey Kuhn‡, and Martin Poenie*§

*Department of Molecular Cell and Developmental Biology, University of Texas, 1 University Station, MC C0930, Austin, TX 78712; †Department of Physiology, University of Pennsylvania, Philadelphia, PA 19104; and ‡Department of Molecular, Cellular, and Developmental Biology, Yale University, New Haven, CT 06520

Edited by Ronald D. Vale, University of California, San Francisco, CA, and approved August 11, 2006 (received for review February 11, 2006)

Binding of T cells to antigen-presenting cells leads to the formation of the immunological synapse, translocation of the microtubule-organizing center (MTOC) to the synapse, and focused secretion of effector molecules. Here, we show that upon activation of Jurkat cells microtubules project from the MTOC to a ring of the scaffolding protein ADAP, localized at the synapse. Loss of ADAP, but not lymphocyte function-associated antigen 1, leads to a severe defect in MTOC polarization at the immunological synapse. The microtubule motor protein cytoplasmic dynein clusters into a ring at the synapse, colocalizing with the ADAP ring. ADAP coprecipitates with dynein from activated Jurkat cells, and loss of ADAP prevents MTOC translocation and the specific recruitment of dynein to the synapse. These results suggest a mechanism that links signaling through the T cell receptor to translocation of the MTOC, in which the minus end-directed motor cytoplasmic dynein, localized at the synapse through an interaction with ADAP, reels in the MTOC, allowing for directed secretion along the polarized microtubule cytoskeleton.

microtubules | T cell polarization | β-catenin | PLAC-24

In T cells, engagement of the T cell receptor leads to formation of an immunological synapse, translocation of the microtubule-organizing center (MTOC) to the synapse, and ultimately secretion of effector molecules (1–4). Translocation of the MTOC serves to focus secretion at the synapse and is required for effector function of both helper and cytotoxic T cells (5–8).

Previous studies have reported that signaling through ZAP-70, LAT, SLP-76, elevation of intracellular calcium, and Cdc42 are required for MTOC translocation (9–12). However, the downstream actions that control MTOC translocation remain to be determined. The microtubule motor cytoplasmic dynein is a good candidate to drive the translocation of the MTOC and the resulting polarization of the microtubule cytoskeleton observed in synapse formation (4). Here, we present data with Jurkat cells showing that a dynein complex is recruited to the synapse and that the recruitment of dynein depends on the protein ADAP. ADAP is a SLP-76-associated scaffold protein that links T cell receptor signaling to integrin clustering through its association with SKAP55 and may also be linked to actin dynamics by virtue of its Ena/vasodilator-stimulated phosphoprotein binding domain (13–18). Here, we show that ADAP is associated with dynein, and upon T cell activation it forms a ring at the synapse that colocalizes with dynein and microtubules. When ADAP expression is reduced by using antisense morpholino (MO) oligonucleotides, dynein fails to localize to the synapse and MTOC translocation is blocked. Together, these results show a direct connection between T cell signaling, recruitment of dynein to the synapse, and polarization of the microtubule cytoskeleton.

Results

Previous studies showed that microtubules project toward a ring of lymphocyte function-associated antigen 1 (LFA-1) clustered at the immunological synapse (4). We used LFA-1-deficient Jurkat cells to test whether LFA-1 is required for MTOC translocation. When LFA-1-deficient Jurkat cells (JB2.7 cell line; ref. 19) were stimulated by *Staphylococcus* enterotoxin E (SEE)-coated Raji cells, normal MTOC polarization was observed (see Fig. 6, which is published as supporting information on the PNAS web site), indicating that LFA-1 is not required for normal synapse formation.

Given the association between ADAP and LFA-1 clustering, we next examined whether the close association between microtubules and sites where LFA-1 was clustered might be caused by ADAP. We first compared the 3D distribution of ADAP to that of LFA-1 in normal Jurkat cells mixed with SEE-coated Raji cells and immunostained for both LFA-1 and ADAP. LFA-1 and ADAP form closely spaced, but distinct, rings at the synapse with the LFA-1 ring interior of the ADAP ring (Fig. 1 *a–d*). All ADAP staining observed in Jurkat–Raji pairs originates from the Jurkat T cells and not the Raji B cells, as B cells do not express ADAP (20).

In unstimulated Jurkat cells, ADAP is clustered around the MTOC and along microtubules extending from the MTOC to the periphery, indicating that it might be associated with microtubules (Fig. 1 *e–g*). Computerized 3D reconstructions of SEE-activated Jurkat–Raji pairs show that virtually all microtubules projecting from the MTOC to the synapse colocalize with the ADAP ring (Fig. 1*h* and Movie 1, which is published as supporting information on the PNAS web site). Often, microtubules appear to adhere to the ring, turning to closely follow the contour of the ADAP surface. Similar results were obtained with human primary T cells (Fig. 7, which is published as supporting information on the PNAS web site).

To determine whether the ADAP ring still formed in the absence of either intact microtubules or LFA-1, we mixed SEE-coated Raji cells with either Jurkat cells treated with 10 μM colchicine to depolymerize microtubules or LFA-1-deficient (JB2.7) Jurkat cells and immunostained for ADAP alone or ADAP and tubulin. Computerized 3D reconstructions show that the absence of either microtubules or LFA-1 had no effect on ADAP ring formation. Additionally, the lack of LFA-1 in JB2.7 cells did not visibly alter the arrangement of microtubules (Fig. 1 *i–l* and Movie 2, which is published as supporting information on the PNAS web site).

Given the close correlation between ADAP and microtubules at the synapse we next sought to determine whether ADAP

Author contributions: J.C. and S.J.K. contributed equally to this work; M.P. designed research; J.C., S.J.K., and S.T. performed research; L.A.L., E.L.F.H., and J.K. contributed new reagents/analytic tools; J.C., S.J.K., E.L.F.H., J.K., and M.P. analyzed data; and J.C., E.L.F.H., and M.P. wrote the paper.

The authors declare no conflict of interest.

This paper was submitted directly (Track II) to the PNAS office.

Abbreviations: DIC, dynein intermediate chain; MTOC, microtubule-organizing center; SEE, *Staphylococcus* enterotoxin E; LFA-1, lymphocyte function-associated antigen 1; MO, morpholino; CTB, Cell Tracker blue.

§To whom correspondence should be addressed. E-mail: poenie@mail.utexas.edu.

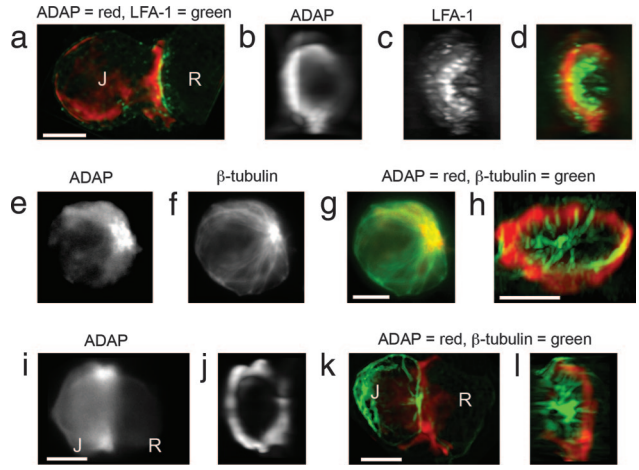

Fig. 1. ADAP, LFA-1, and microtubules at the Jurkat immunological synapse. (*a–d*) SEE-coated Raji (R) cells conjugated to Jurkat (J) cells were fixed and immunostained for LFA-1 and ADAP. The *z*-axis stacks (256 images) were acquired for LFA-1, and ADAP fluorescence data were processed as described (3). A Jurkat–Raji pair immunostained for ADAP (red) and LFA-1 (green) is shown from a side view (*a*) and facing the synapse with separate panels for ADAP (*b*) and LFA-1 (*c*). A red–green overlay of the data from *b* and *c* is shown in *d*. Note that the ADAP and LFA-1 rings are separate and distinct. (*e–g*) Jurkat cells were immunostained for ADAP (*e*) and tubulin (*f*) with the red–green overlay shown in *g* (red, ADAP; green, tubulin). (*h*) SEE-coated Raji cells pretreated with colchicine to depolymerize microtubules were mixed with normal Jurkat cells and then immunostained for tubulin (green) and ADAP (red). Image stacks were acquired and processed as for *a–d*. A typical Jurkat–Raji pair shows microtubules projecting from the MTOC to the ADAP ring where the microtubules often closely follow its surface. A rotatable view is available as Movie 1. (*i–j*) Cells were prepared identically to the procedure in *a–d* except that Jurkat cells were pretreated with 10 μM colchicine to depolymerize the microtubules. The results show that the ADAP ring forms in the absence of an intact microtubule cytoskeleton. (*k* and *l*) Cells were prepared identically to the procedure in *a–d* except that JB2.7 (LFA-1-deficient) Jurkat cells were used in place of normal Jurkat cells. The results show that microtubules are associated with a typical ADAP ring in the absence of LFA-1. Data are representative of two to three independent experiments. (Scale bars: 5 μm.)

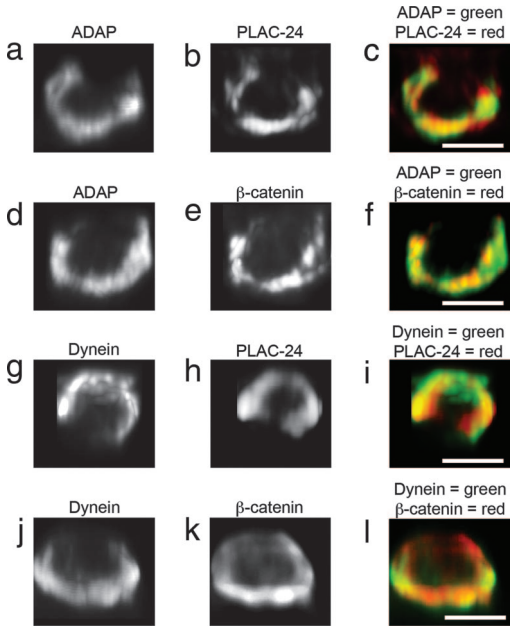

Fig. 3. The spatial relationship between ADAP, dynein, PLAC-24, and β-catenin at the synapse. Jurkat–Raji cell pairs were fixed, immunostained, and subsequently processed by computerized 3D reconstruction as described. (*a–c*) A Jurkat–Raji pair is immunostained for ADAP (*a*) and PLAC-24 (*b*) with the red–green overlay shown in *c*. (*d–f*) A Jurkat–Raji pair is immunostained for ADAP (*d*) and β-catenin (e) with the red–green overlay shown in *f*. (*g–i*) A Jurkat–Raji pair is immunostained for dynein using mAb 70.1 (*g*) and PLAC-24 (*h*) with the red–green overlay shown in *i*. (*j–l*) A Jurkat–Raji pair is immunostained for dynein using mAb 70.1 (*j*) and β-catenin (*k*) with the red–green overlay shown in *l*. Data are representative of three independent experiments. (Scale bars: 5 μm.)

immunoprecipitates with dynein. Cytoplasmic dynein was immunoprecipitated from Jurkat–Raji mixtures with or without SEE stimulation by using an affinity-purified polyclonal rabbit antibody (1467) to the dynein intermediate chain (DIC; antibody specificity is shown in Fig. 8, which is published as supporting information on the PNAS web site). Western blots of immunoprecipitates from both unstimulated and stimulated lysates were probed for dynein (Fig. 2*a Top*) and ADAP (Fig. 2*a Middle*). The results show that substantially more dynein is pulled down in activated as compared with the nonactivated Jurkat lysates. This difference is not caused by a change in dynein expression levels because both 70.1 (Fig. 2*a*) and 1467 (Fig. 2*b*) recognize the same

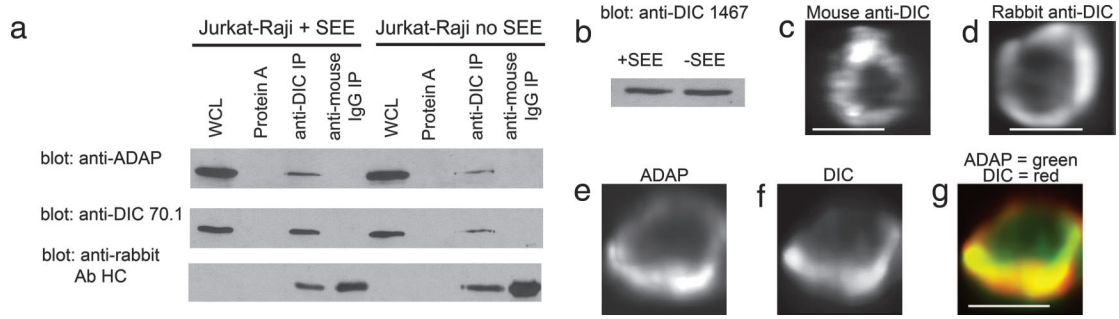

Fig. 2. A dynein complex clusters at the immunological synapse and associates with ADAP. (*a*) To determine whether ADAP is bound to dynein, rabbit anti-DIC 1467 was used to immunoprecipitate (IP) dynein from homogenates of SEE-stimulated or unstimulated Jurkat–Raji mixtures. The immunoprecipitate was then probed on separate blots with mouse anti-ADAP mAb and mouse anti-DIC mAb 70.1. The results show an increase in both ADAP (*Top*) and dynein (*Middle*) in the activated compared with nonactivated Jurkat lysates. (*Bottom*) Levels of antibody in the IP are shown. No ADAP or dynein is detected when specific antibody is replaced with beads alone or beads bound to rabbit anti-mouse Ig. Similar amounts of total dynein and ADAP were detected in the whole-cell lysates (WCL). (*b*) The whole-cell lysates from *a* were also probed with anti-DIC 1467. The results show that 1467 recognizes similar levels of dynein in the activated and nonactivated Jurkat lysates. (*c* and *d*) Computerized 3D reconstructions of fluorescence data were prepared from Jurkat/SEE-coated Raji conjugates fixed and immunostained with anti-DIC mAb 70.1 (*c*) or rabbit anti-DIC 1467 (*d*). Both antibodies show a ring-like staining pattern at the Jurkat-Raji immunological synapse. (*e* and *f*) The same procedures as in *c* and *d* were then used to examine Jurkat–Raji pairs immunostained for ADAP (*e*) and dynein with mAb 70.1 (*f*). (*g*) The red-green-blue overlay shows DIC colocalizes with ADAP at the synapse. Data are representative of three independent experiments. (Scale bars: 5 μm.)

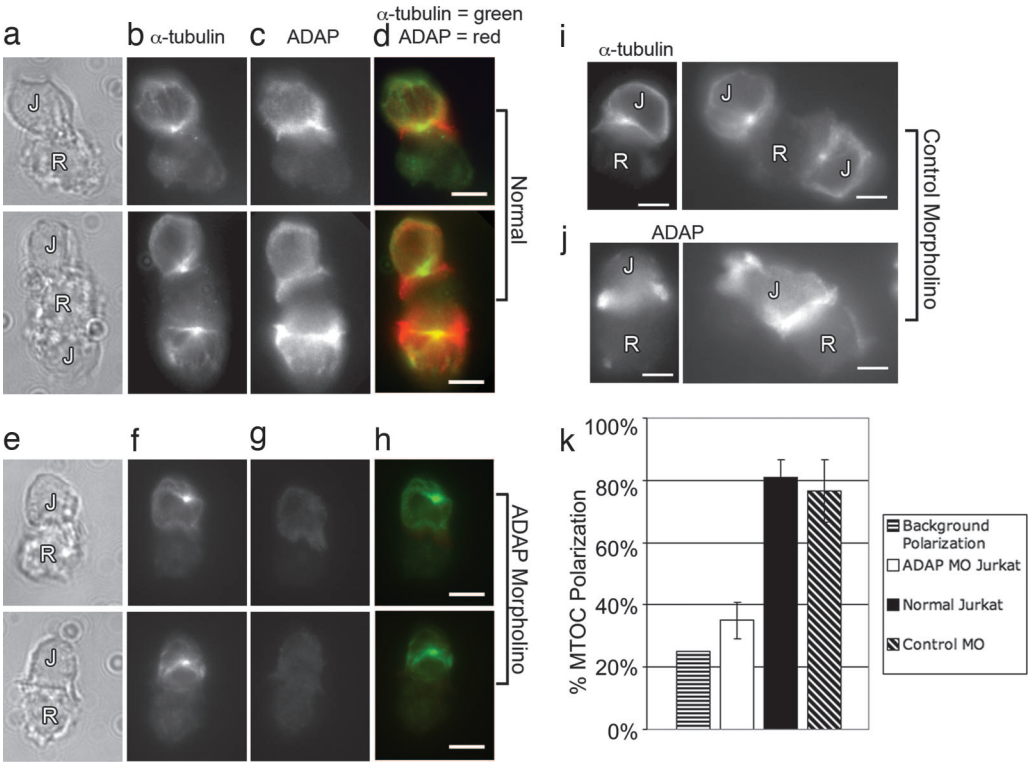

Fig. 4. MO-mediated ADAP knockdown abolishes MTOC polarization in Jurkat cells. Jurkat cells were electroporated with either an antisense MO directed against ADAP (ADAP MO) or a standard control MO 24 h before experiment. Normal (untreated), ADAP MO, and control MO Jurkat cells were used in the preparation of Jurkat (J)–Raji (R) cell pairs as described. (*a–d*) Normal Jurkat–Raji pairs shown in bright field (*a*) were immunostained for α-tubulin (*b*) and ADAP (mouse anti-fyb, clone 5) (*c*) with the red–green overlay shown in *d*. The results show typical ADAP clustering and MTOC polarization. (*e–h*) ADAP MO-treated Jurkat–Raji pairs prepared as in *a–d* show a loss of ADAP from the synapse and failure of MTOC polarization. (*i–j*) Control MO prepared as in *a–d* show normal ADAP clustering and normal MTOC polarization. (*k*) A bar graph summarizing polarization counts demonstrates a dramatic reduction in MTOC polarization in the ADAP MO Jurkat cells compared with normal and control MO Jurkat cell preparations. Note that background polarization levels obtained by treating Jurkat cells with the Srk kinase inhibitor PP2 are 25%. Data are representative of three independent experiments. Normal, $n = 50$ cell pairs; control MO, $n = 50$ cell pairs; ADAP MO, $n = 50$ cell pairs. Error bars represent ± SD. (Scale bars: 5 μm.)

amount of dynein in blots of the whole-cell lysates. ADAP coprecipitates with dynein in both activated and nonactivated lysates in amounts that are proportional to the amount of dynein. Neither protein A beads alone or bound to rabbit anti-mouse as a control showed any tendency to pull down ADAP or dynein (Fig. 2*a Bottom*).

We next sought to localize dynein in SEE-stimulated Jurkat–Raji pairs. Dynein immunostains using either 70.1 mAb (Fig. 2*c*) or 1467 (Fig. 2*d*) showed that dynein formed a ring-like structure at the synapse similar to that of ADAP. Jurkat–Raji pairs were then immunostained with antibodies to both ADAP (Fig. 2*e*) and dynein (Fig. 2*f*); the overlay (Fig. 2*g*) shows that ADAP and dynein colocalize as rings at the synapse. Normally the MTOC is located roughly in the center of the ADAP and dynein rings, but when partial rings form the MTOC is shifted over to the site where ADAP or dynein are clustered (see Fig. 9, which is published as supporting information on the PNAS web site). This spatial correlation suggests a functional relationship between the clustering of ADAP, dynein, and movements of the MTOC.

Two proteins, PLAC-24 and β-catenin, have been proposed to anchor dynein at actin-rich adherens junctions (21, 22) and potentially could serve a similar role in linking dynein to the immunological synapse. Furthermore, Western blots indicated that both PLAC-24 and β-catenin are expressed in Jurkat cells (see Fig. 10, which is published as supporting information on the PNAS web site). When Jurkat–Raji pairs were immunostained for ADAP, dynein, PLAC-24, and β-catenin (Fig. 3), the results showed that these proteins all localize to the same ring-like structure.

We next sought to determine whether loss of ADAP altered the distribution of dynein at the synapse. ADAP expression was reduced in Jurkat cells with an antisense MO oligonucleotide complementary to the first 25 nt of ADAP mRNA (beginning with the start codon). MOs were introduced into cells by electroporation with a transfection efficiency in the range of 75–85% as determined with a FITC standard control MO (see Fig. 11, which is published as supporting information on the PNAS web site). Verification of ADAP knockdown was performed by Western blot of cell lysates from normal Jurkat cells and those transfected with either a standard control MO or ADAP MO. Bulk ADAP expression in MO-treated cells was reduced by 50% as compared with either untreated cells or control cells.

To determine whether the formation of the ADAP ring is necessary for MTOC polarization, colchicine-pretreated, SEE-coated Raji cells were mixed with normal, ADAP MO, and control MO Jurkat cells and were fixed and immunostained for ADAP and tubulin (Fig. 4 *a–j*). ADAP MO cell pairs were chosen as those having Jurkat cells with little to no ADAP expression as determined by ADAP immunostaining. Comparison of MTOC polarization in normal, ADAP MO, and control MO Jurkat cells gave scores of 81% ± 6 (normal), 77% ± 10 (control MO), and 35% ± 6 (ADAP MO) (counts from three independent experiments with 50 cell pairs counted per experiment) (Fig. 4*k*). Background polarization values of

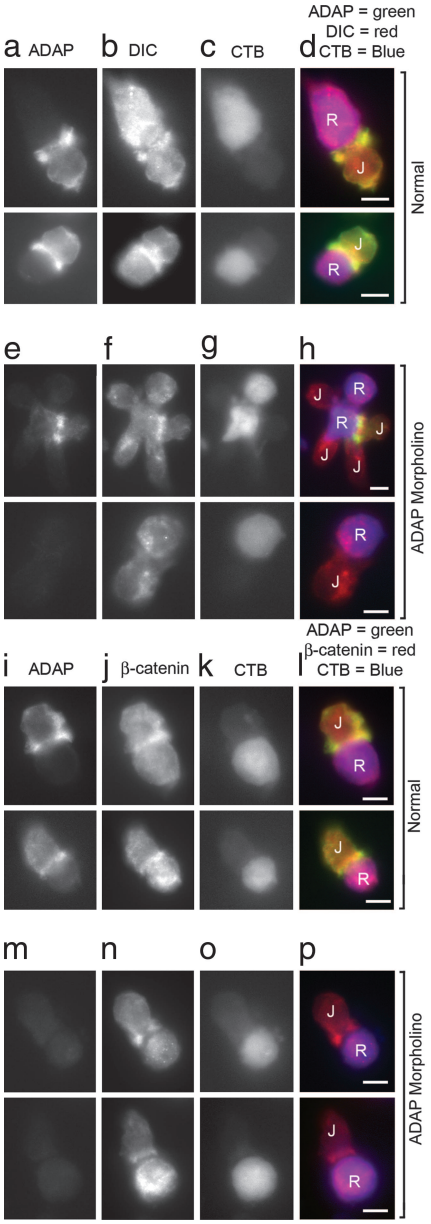

Fig. 5. MO-mediated ADAP knockdown abolishes synaptic dynein clustering but not β-catenin clustering in Jurkat (J) cells. Raji (R) cells were labeled with CTB, and both untreated (normal) and ADAP MO Jurkat–Raji cell pairs were prepared and immunostained as described. (*a–d*) Normal Jurkat–Raji pairs with Raji cells labeled with CTB were immunostained for ADAP (mouse anti-fyb, clone 5) (*a*), DIC (rabbit anti-DIC 1467) (*b*), and CTB (*c*); the red–green–blue overlay (*d*) shows typical ADAP and DIC clustering at the synapse. (*e–h*) Experiments parallel to those shown in *a–d* were carried out by using CTB-labeled Raji cells and ADAP-MO-treated Jurkat cells. Note that in the top row, there were four Jurkat cells bound to the central Raji cell. One of these cells still expressed ADAP after ADAP-MO electroporation and this cell shows dynein was also clustered at the synapse. The remaining cells show little or no ADAP or dynein at the synapse. (*i–p*) Normal (*i–l*) and ADAP MO (*m–p*) Jurkat–Raji pairs with Raji cells labeled with CTB were immunostained for ADAP (mouse anti-fyb, clone 5) (*i* and *m*) and β-catenin (rabbit anti-β-catenin) (*j* and *n*). The red–green–blue overlays (*l* and *p*) show typical β-catenin clustering at the synapse in both normal and ADAP MO Jurkat cells. Data are representative of two to three independent experiments. (Scale bars: 5 μm.)

≈25% were obtained by using the Src kinase inhibitor PP2 to block Jurkat activation. These results demonstrate a severe defect in MTOC polarization in Jurkat cells lacking ADAP.

To ensure that the ADAP MO Jurkat cells still activate normally, Cell Tracker blue (CTB)-labeled, SEE-coated Raji cells were mixed with normal and ADAP MO Jurkat cells, fixed, and immunostained for ADAP and phospho-LAT. The results demonstrate normal clustering of phospho-LAT in cells lacking ADAP expression (see Fig. 12, which is published as supporting information on the PNAS web site).

To determine how loss of ADAP impacts the recruitment of dynein to the synapse, CTB-labeled, SEE-coated Raji cells were mixed with either normal or ADAP-MO Jurkat cells, fixed, and immunostained for ADAP and DIC. Normal cell pairs exhibited typical coclustering of ADAP and DIC at the synapse (Fig. 5 *a–d*), but ADAP MO Jurkat cells with little to no ADAP (as judged by fluorescence microscopy) also showed an absence of DIC at the synapse. This is clearly evident in Fig. 5 *e–h Upper*, where of the four Jurkat cells in contact with the central Raji cell, the only synapse with dynein clustered is also the only cell with detectable ADAP at the synapse. Thus, loss of ADAP also results in a failure to recruit dynein to the synapse. In contrast, β-catenin (Fig. 5 *i–p*), PLAC-24, and actin (see Fig. 13, which is published as supporting information on the PNAS web site) still clustered at the synapse in both normal and ADAP MO cells. These data suggest that β-catenin and PLAC-24 clustering occurs independently of ADAP and that gross synapse structure remains largely intact.

Discussion

Our studies of Jurkat cells show that upon activation by SEE-coated Raji cells both ADAP and dynein move to the synapse where they colocalize in the form of a ring. ADAP coimmunoprecipitates with dynein, suggesting that these proteins associate either directly or indirectly; this association is enhanced in activated cells. It is interesting to note that the dynein ring at the synapse represents a subpopulation of the total cellular pool, which is selectively labeled by specific antidynein antibodies (UP1467, mAb 70.1). This selective labeling may arise from differential unmasking of the epitope, possibly arising from changes in dynein binding proteins that occur upon activation of Jurkat cells.

Recruitment of dynein to the synapse provides a plausible model for how MTOC translocation is accomplished. Dynein may be specifically recruited to the ADAP ring upon activation. Once anchored through the ADAP interaction, synaptic dynein would generate tension on microtubules, causing them to slide along the cortex while reeling the MTOC toward the synapse. This model is consistent with the observed motions of the MTOC and the microtubule sliding seen with modulated polarization microscopy (ref. 4 and see Fig. 14 and Movie 3, which are published as supporting information on the PNAS web site). In particular, the large oscillations of the MTOC between two contact sites implies a microtubule sliding mechanism. Furthermore, microtubules are observed bending in the same direction as bulk MTOC movement and maintaining their length while sliding along the cortex (Fig. 11), further implicating dynein in these movements. Our data establish a role for dynein in this process, as we show that loss of ADAP prevents recruitment of dynein and translocation of the MTOC.

ADAP provides an important connection to the T cell activation pathway through its linkage to SLP-76 (18, 23, 24) and to the actin cytoskeleton through its Ena/vasodilator-stimulated phosphoprotein (VASP)-binding domain (16), although loss of ADAP or mutation of its Ena/VASP-binding domain does not prevent actin polymerization or synapse formation (13, 23). The relationship between ADAP, the actin cytoskeleton, and dynein seemed to fit nicely with the observation that PLAC-24 and β-catenin are similarly recruited to the synapse. In epithelial cells, Karki *et al.* (21) and Ligon *et al.* (22) showed that the dynein binds to β-catenin and PLAC-24 at an actin-rich adherens

junction. However, we found that loss of ADAP did not block recruitment of PLAC-24 or β-catenin, indicating that they are not sufficient alone to recruit dynein to the synapse. We also found that LFA-1 was not required for recruitment of dynein despite previous studies of mouse T cells showing a close correlation between sites where microtubules and LFA-1 are clustered at the synapse (4). Here, using Jurkat cells, we see a similar close correlation between location of microtubules and the MTOC and sites where ADAP and dynein are clustered. However, mouse and human cells differ in the spatial relationship between ADAP, dynein, and LFA-1 at the synapse and in the observation that ADAP is not required for MTOC translocation in mouse T cells (J.C., S.K., and M.P., unpublished observations). Further studies will be required to address these differences at the mechanistic level.

Methods

Antibodies, Cell Lines, and Reagents. RPMI medium 1640, glutamine, and sodium pyruvate were purchased from Invitrogen (Carlsbad, CA). Heat- inactivated FBS was obtained from Atlas Biologicals (Fort Collins, CO). Partially purified SEE was purchased from Toxin Technology (Sarasota, FL). Polylysine (58 kDa), Tween-20, Triton X-100, EDTA, protein G, FITC-phalloidin, and colchicine were purchased from Sigma (St. Louis, MO). Paraformaldehyde and glyoxal were purchased from Aldrich (Milwaukee, WI). CTB and ProLong Gold Antifade mounting media were purchased from Molecular Probes (Eugene, OR). All other reagents used in this study were of the highest quality available.

The antibodies used in this study were as follows: mouse antitubulin IgG clone TUB 2.1 (T4026; Sigma), mouse anti-DIC IgM clone 70.1 (ref 25; D5167; Sigma), mouse anti-DIC IgG clone 74.1 (ref. 25; MMS-400P; Covance, Princeton, NJ), mouse anti-CD11a (LFA-1) IgG clone TS1/22 (ref. 26; MA11A10; Endogen-Pierce, Rockford, IL), mouse anti-fyb (ADAP) IgG clone 5 (ref. 20; 610945; BD Biosciences, San Diego, CA), rat anti-α-tubulin IgG clone YOL 1/34 (CBL270; Chemicon, Temecula, CA), rabbit anti-β-catenin (ref. 27; 06-734; Upstate Biotechnology, Lake Placid, NY), rabbit anti-phospho-LAT Tyr-191 (3584S; Cell Signaling, Beverly, MA), FITC-labeled rat anti-mouse IgG (RMG101; Caltag Laboratories, Burlingame, CA), FITC-labeled goat anti-mouse IgG antibody (F0257; Sigma), red X-labeled goat anti-mouse IgG (115-295-166; Jackson ImmunoResearch, West Grove, PA), TRITC-labeled bovine anti-goat IgG (sc2349; Santa Cruz Biotechnology, Santa Cruz, CA), TRITC goat anti-mouse IgG-Fc specific (T7657; Sigma), FITC goat anti-mouse IgM-μ specific (F9259; Sigma), and Alexa Fluor 594-conjugated goat anti-rabbit IgG (A-11037; Molecular Probes). The rabbit anti-DIC (1467, see Fig. 7) and rabbit anti-PLAC-24 antibodies were developed by E.L.F.H. The sheep anti-ADAP antibody was a generous gift from Gary Koretzky (University of Pennsylvania School of Medicine, Philadelphia, PA) (18).

Normal Jurkat (clone E6-1) and Raji cells were obtained from ATCC, Manassas, VA. LFA-1-deficient Jurkat cells (JB2.7) were acquired as a gift from Timothy Springer (Harvard Medical School, Boston, MA). Jurkat, Raji, and EL4.BU cells were grown at 37°C (5% CO_2) in RPMI medium 1640 containing 10% heat-inactivated FBS, 50 μM β-mercaptoethanol, 24 mM $NaHCO_3$, 1 mM pyruvate, and 1 mM glutamine. The Jurkat and Raji cells were cultured in a 37°C incubator with 5% CO_2.

MO-Mediated Knockdown of ADAP in Jurkat Cells. For each electroporation, 2×10^7 cells were suspended in 400 μl of RPMI medium 1640, and 15 nmol of MO was incubated with cells for 15 min at room temperature. The suspension was electroporated in a 4-mm cuvette by using a Bio-Rad (Hercules, CA) Gene Pulser II (950 mF and 250 V). The cells were immediately transferred to 10 ml of growth medium.

MO Sequences. ADAP MO (TGCCCCCCGTGTTATATTTC-GCCAT) (complementary to nucleotides 1–25 of human ADAP), and FITC-labeled standard control MO (CCTCTTAC-CTCAGTTACAATTTATA) were purchased from Gene Tools (Philomath, OR).

Preparation of Jurkat–Raji Conjugates. Raji cells were incubated for 1.5 h with 2 μg/ml of partially purified SEE before mixing with Jurkat cells. To distinguish between Raji and Jurkat cells, the Raji cells were treated either with colchicine (10 μM final) or CTB (1 μM) during the last 15 min of the SEE incubation period. Jurkat and Raji cells were washed by centrifugation, mixed, and pelleted together. For immunostaining, the pellet was resuspended in RPMI media 1640 and plated on polylysine-coated coverslips where they were allowed to adhere for 15 min before fixation.

Cell Lysis and Immunoprecipitation. To prepare cell lysates, cells were pelleted, mixed with 1 ml of ice-cold lysis buffer containing 25 mM Tris (pH 8.0), 50 mM NaCl, 0.5% Triton X-100, 2 mM EDTA, 50 mM NaF, 1 mM $NaVO_4$, 1 mM PMSF, 1 mg/ml leupeptin, 1 mg/ml aprotinin, and 1 mg/ml pepstatin, homogenized by passage through a 21-ga syringe, and cleared by microcentrifugation (250 × *g* for 10 min). The supernatant was precleared with protein G beads for 1.5 h at 4°C followed by centrifugation and then incubated with control or precipitating antibody (prebound to protein G beads) for 3 h at 4°C. Subsequently, the protein G beads were pelleted by centrifugation and washed three times in lysis buffer and resolved by SDS/PAGE.

Western Blots of SDS/PAGE Gels. Gel electrophoresis and transfers were carried out with a Bio-Rad Miniprotean apparatus. Proteins from SDS/PAGE gels were transferred to 0.2-μm nitrocellulose membrane (Bio-Rad), blocked in a solution of 5% powdered milk in Tris-buffered saline (25 mM Tris/137 mM NaCl/2.7 mM KCl/0.025% Tween-20, pH 7.4), and incubated with antibodies essentially as described by the manufacturer. The labeled blots were developed with a Pierce Super Signal Pico detection kit.

Antibody Staining. Jurkat–SEE-Raji pairs were fixed in 3% formaldehyde or 2% formaldehyde with 1% glyoxal for 30 min on coverslips and then imaged by using essentially the same procedures as described (4).

We thank Gary Koretzky for helpful discussions and generous provision of reagents. This work was supported by National Institutes of Health Grant AA15437 (to M.P.). J.C. was supported by National Science Foundation Integrative Graduate Education and Research Traineeship Grant DGE-9870653. L.A.L. and E.L.F.H. were supported by National Institutes of Health Grant GM068591.

1. Poenie M, Kuhn JR, Combs J (2004) *Curr Opin Immunol* 16:428–438.
2. Monks CR, Freiberg BA, Kupfer H, Sciaky N, Kupfer A (1998) *Nature* 395:82–86.
3. Kupfer A, Dennert G (1984) *J Immunol* 133:2762–2766.
4. Kuhn JR, Poenie M (2002) *Immunity* 16:111–121.
5. Kupfer A, Swain SL, Janeway CA, Jr, Singer SJ (1986) *Proc Natl Acad Sci USA* 83:6080–6083.
6. Kupfer H, Monks CR, Kupfer A (1994) *J Exp Med* 179:1507–1515.
7. Poo WJ, Conrad L, Janeway CA, Jr (1988) *Nature* 332:378–380.
8. Stinchcombe JC, Bossi G, Booth S, Griffiths GM (2001) *Immunity* 15:751–761.
9. Lowin-Kropf B, Shapiro VS, Weiss A (1998) *J Cell Biol* 140:861–871.
10. Blanchard N, Di Bartolo V, Hivroz C (2002) *Immunity* 17:389–399.
11. Kuhne MR, Lin J, Yablonski D, Mollenauer MN, Ehrlich LI, Huppa J, Davis MM, Weiss A (2003) *J Immunol* 171:860–866.
12. Stowers L, Yelon D, Berg LJ, Chant J (1995) *Proc Natl Acad Sci USA* 92:5027–5031.
13. Peterson EJ, Woods ML, Dmowski SA, Derimanov G, Jordan MS, Wu JN, Myung PS, Liu QH, Pribila JT, Freedman BD, *et al.* (2001) *Science* 293:2263–2265.
14. Rudd CE, Wang H (2003) *Am J Transplant* 3:1204–1210.

15. Huang Y, Norton DD, Precht P, Martindale JL, Burkhardt JK, Wange RL (2005) *J Biol Chem* 280:23576–23583.
16. Krause M, Sechi AS, Konradt M, Monner D, Gertler FB, Wehland J (2000) *J Cell Biol* 149:181–194.
17. Liu J, Kang H, Raab M, da Silva AJ, Kraeft SK, Rudd CE (1998) *Proc Natl Acad Sci USA* 95:8779–8784.
18. Musci MA, Hendricks-Taylor LR, Motto DG, Paskind M, Kamens J, Turck CW, Koretzky GA (1997) *J Biol Chem* 272:11674–11677.
19. Weber KS, York MR, Springer TA, Klickstein LB (1997) *J Immunol* 158: 273–279.
20. da Silva AJ, Li Z, de Vera C, Canto E, Findell P, Rudd CE (1997) *Proc Natl Acad Sci USA* 94:7493–7498.
21. Karki S, Ligon LA, DeSantis J, Tokito M, Holzbaur EL (2002) *Mol Biol Cell* 13:1722–1734.
22. Ligon LA, Karki S, Tokito M, Holzbaur EL (2001) *Nat Cell Biol* 3: 913–917.
23. Wang H, McCann FE, Gordan JD, Wu X, Raab M, Malik TH, Davis DM, Rudd CE (2004) *J Exp Med* 200:1063–1074.
24. Raab M, Kang H, da Silva A, Zhu X, Rudd CE (1999) *J Biol Chem* 274:21170–21179.
25. Dillman JF, 3rd, Pfister KK (1994) *J Cell Biol* 127:1671–1681.
26. Hill S, Milla PJ, Ciampolillo A, Napolitano G, Bottazzo GF, Mirakian R (1992) *Autoimmunity* 13:233–241.
27. Knudsen KA, Soler AP, Johnson KR, Wheelock MJ (1995) *J Cell Biol* 130:67–77.